




Efficient Constraint Handling Technique-Based Beamformer for Advanced Antenna Systems

L. T. Trang ^{1,2}, N. V. Cuong ¹, and T. V. Luyen ^{1,*}

¹ Faculty of Electronic Engineering, Hanoi University of Industry, Hanoi, Vietnam

² Faculty of Electronics and Telecommunications, Electric Power University, Hanoi, Vietnam

Email: tranglt@hau.edu.vn (L.T.T.); cuongnv@hau.edu.vn (N.V.C.); luyentv@hau.edu.vn (T.V.L.)

*Corresponding author

Abstract—This paper introduces an advanced beamformer that utilizes Constraint Handling Techniques (CHTs) and metaheuristic algorithms for pattern nulling in a Uniformly Spaced Linear Array (ULA), effectively positioning imposed nulls in the directions of interference. We explore four scenarios of ULA patterns with preset nulls, employing the Adaptive Penalty Technique (APT) and comparing the results with the Original Feasibility Rules Technique (OFRT) to validate our approach. The proposed beamformer, utilizing CHTs, demonstrates remarkable capabilities in suppressing side beams, maintaining a predetermined beam width, and accurately placing single, multiple, and broad nulls at arbitrary interference directions. Additionally, our findings indicate that the beamformer using APT is more efficient than the one using OFRT, particularly in terms of convergence speed during sample synthesis. This study underscores how integrating CHTs with metaheuristic algorithms enhances the optimization of beamforming in advanced antenna systems, thereby improving signal processing and communication system performance in various real-world applications.

Keywords—constraint handling techniques, uniformly spaced linear array, null-steering, adaptive penalty technique, original feasibility rules technique

I. INTRODUCTION

In the realm of signal processing and telecommunications, advanced antenna systems, particularly beamforming techniques, play a pivotal role in enhancing the performance of wireless communication networks. Beamforming has garnered significant attention in Uniform Linear Array (ULA) systems due to its ability to precisely direct transmitted or received signals, thereby amplifying their strength, minimizing interference, and boosting overall system capacity. ULAs are widely utilized in beamforming due to their simplicity and effective performance [1]. The essence of beamforming lies in manipulating signals from individual antenna elements based on predefined principles, aiming to sculpt and guide the array's beam to achieve objectives such as steering the main beam in a desired direction, adjusting sidelobe levels, and creating null regions. This technique

enables the antenna array to form and control its beams to meet specific communication system requirements [2].

Optimizing beamforming in ULA systems, however, entails addressing complex constraint optimization problems that must consider practical factors such as hardware limitations, regulatory requirements, and specific system specifications. One critical challenge in this optimization process is effectively managing the multitude of constraints imposed by these considerations. Constraint Handling Techniques (CHTs) emerge as powerful tools within the framework of metaheuristic optimization algorithms, facilitating efficient navigation of complex solution spaces while ensuring compliance with all relevant constraints. By incorporating specialized mechanisms for constraint handling, CHTs empower metaheuristics to address and overcome the intricate challenges inherent in optimizing beamforming for advanced antenna systems [3].

Metaheuristic algorithms, including the Grey Wolf Optimizer (GWO), Genetic Algorithms, Multi-Verse Optimizer, and Artificial Bee Colony, offer powerful optimization tools for beamforming in antenna arrays [4]. However, integrating these metaheuristics with beamforming presents challenges, particularly in handling constraints inherent in practical beamforming problems. These constraints may include steering angle constraints, power constraints, element spacing constraints, and mutual coupling constraints, among others. CHTs play a crucial role in optimization algorithms, particularly when dealing with constrained optimization problems. Here are some general characteristics and strengths of these techniques:

- Flexibility in handling constraints: Metaheuristic algorithms can handle both equality and inequality constraints more flexibly compared to convex approximation methods. These algorithms can integrate various CHTs, such as penalty methods, constraint dominance, repair mechanisms, or constraint satisfaction, directly into the optimization process [5].
- Adaptability to problem structure: Metaheuristic algorithms can be easily adapted to problem-specific structures and characteristics. They can leverage knowledge about the problem to develop custom

operators, problem-specific search strategies, and combinations with other optimization methods that are more effective for hard, non-convex problems [6, 7].

- Handling multi-objective optimization: Metaheuristic optimization algorithms naturally lend themselves to solving multi-objective optimization problems (MOPs) by maintaining a diverse set of solutions (Pareto fronts) representing trade-offs between conflicting objectives. Techniques such as dominance, diversity preservation, and elitism are commonly employed to effectively tackle MOPs [8].
- Robustness to problem complexity: Metaheuristic algorithms demonstrate robust performance across a wide range of problem complexities and dimensions. They do not rely on assumptions of convexity or smoothness, making them suitable for highly non-linear, non-convex, and discontinuous objective functions [9].

In summary, while convex approximation methods like geometric programming or successive convex approximation have their advantages in certain scenarios, CHTs using metaheuristic optimization provide a more versatile and robust approach for solving non-convex problems, multi-objective optimization problems, and constrained problems [10].

Integration with metaheuristics: CHTs are often seamlessly integrated with metaheuristic optimization algorithms. This integration enhances the ability of metaheuristics to explore and exploit the solution space while respecting constraints. CHTs using metaheuristic optimization offer several advantages compared to convex approximation methods such as geometric programming or sequential successive convex approximation when solving non-convex problems, multi-objective optimization problems, and constrained problems [6]. CHTs help optimization algorithms uncover high-quality, workable solutions in a variety of application domains by utilizing these traits and strengths to efficiently manage limited optimization issues.

Many researchers have created, improved, and evaluated numerous CHTs implemented in specific metaheuristic optimization algorithms (MOAs) for optimization problems. Researchers have applied CHTs across various fields, especially focusing on MOAs, such as studying the evaluation and performance analysis of CHTs using advanced algorithms in 2002 [11]. By 2011, researchers had thoroughly examined and extensively incorporated CHTs into nature-inspired algorithms, such as EA or those derived from swarm intelligence [12]. These methods include feasibility rules, electronic constraint techniques, stochastic ranking, penalty methods, multi-objective concepts, special operators, and composite CHTs. In 2015, research and evaluation focused on penalty-based CHTs, combining particle swarm optimization with other optimization methods [13]. Electronic constraint techniques, penalty functions, feasibility rules, and stochastic ranking CHTs were all scrutinized in depth in a 2018 review [14] of the

Differential Evolution algorithm, with a focus on benchmark dynamic conic optimization problems.

To address continuous optimization problems, the GWO metaheuristic method was employed. The GWO algorithm draws inspiration from the social structure and hunting tactics observed in gray wolves. The algorithm mimics the hierarchical leadership structure and cooperative hunting tactics of a wolf pack to solve optimization problems. It offers advantages such as simplicity, fast convergence, and effectiveness in handling both continuous and discrete optimization problems [15].

This paper presents a beamformer proposal based on CHTs to construct a suitable objective function combined with metaheuristic optimization. Although some authors have applied a number of separate CHTs in the synthesis of radiation diagrams, such as [16], [17], and [18] in this paper, CHT has been highlighted in the synthesis of diagrams for radiation. This paper elucidates the role of CHTs, specifically assessing two CHTs, APT and OFRT, in the development of an appropriate objective function combined with metaheuristic optimization. For the adaptive control null ULA antenna model, four scenarios will be examined to assess CHTs using beamforming techniques that rely on complex manipulation of the excitation signal's weighting for each element in the antenna array, often employing metaheuristic algorithms. After presenting and analyzing the problem, four simulation scenarios are provided. These include examining the convergence characteristic and putting single, multiple, and wide nulls on the radiation pattern in the ideal case, all of which will be implemented through the null setting technique by modifying complex weights based on the GWO algorithm, the APT, and the OFRT.

II. PROBLEM FORMULATION

This paper examines HDULA, which features a radiation pattern depicted in Fig. 1 and a linear array with uniform spacing, containing M elements arranged along the y axis, also shown in Fig. 1. In this paper, the azimuth angle ϕ will consistently be assumed to be 90° .

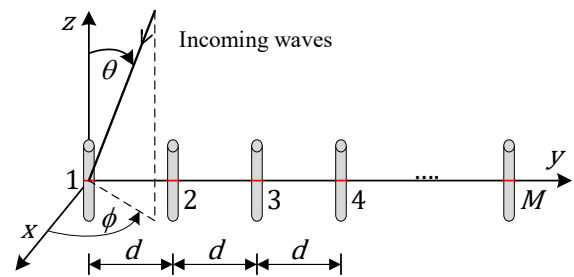


Fig. 1. The array of dipole antennas comprises M elements.

The array's radiation pattern at the corner θ can be represented as follows:

$$\begin{aligned}
 P(\theta) &= EF(\theta) \cdot AF(\theta) \\
 &= EF(\theta) \sum_{m=1}^M w_m e^{j(m-1)\psi}
 \end{aligned} \tag{1}$$

where:

- $EF(\theta)$: represents the element factor of a half-wavelength dipole antenna; AF represents the array factor in the direction θ .
- $\psi = kd \sin(\theta)$; $k = \frac{2\pi}{\lambda}$: the numbers representing the waves; $d = \frac{\lambda}{2}$: the spacing between adjacent elements; and λ : the wavelength.
- $w_m = a_m e^{j\delta_m}$: the complex weight activated at the m -th array element; a_m and δ_m : the amplitude and the phase of the current at the m array element.
- M : The total number of antenna elements in the array.

The array pattern for ULA can be represented as a vector as follows:

$$P(\theta) = EF(\theta) \mathbf{s}(\theta) \mathbf{w} \quad (2)$$

where:

- \mathbf{s} : Steering vectors

$$\mathbf{s}(\theta) = \left[e^{j(n_0\psi_y)}, \dots, e^{j(n_{N-1}\psi_y)} \right] \quad (3)$$

- \mathbf{w} : Complex weight vectors

$$\mathbf{w} = [w_1, \dots, w_N]^T \quad (4)$$

To achieve the desired array pattern with K nulls in the directions (θ_k) , the problem with respect to \mathbf{w} can be expressed as:

$$\begin{aligned} \max_{\mathbf{w}} \quad & P(\theta_0) \\ \text{s.t.} \quad & P(\theta_k) \leq P_{\text{thr}} \quad \forall k = 1, \dots, K \end{aligned} \quad (5)$$

where: P_{thr} is threshold for the desired null-depth level.

During the transmission of electromagnetic energy in an antenna array, the radiation characteristics, including impedance and radiation pattern, of the antenna elements, are affected by the presence of other elements within the array. This phenomenon is known as Mutual Coupling (MC). Mutual coupling plays a crucial role in adaptive arrays as it directly impacts the efficiency and performance of the array, such as the direction of the main lobe, SideLobe Level (SLL), and Null Depth Level (NDL). Therefore, to characterize mutual coupling, Mutual Impedance, Coupling Matrix, S-Parameter, or Embedded Element Patterns have been widely used [19]. The paper will utilize mutual impedance to account for the effects of mutual coupling in a half-wavelength dipole antenna array.

For mutual impedance, if the source voltages $\mathbf{V} = [V_1 \ V_2 \ \dots \ V_M]^T$ are known, the input currents (excitation weights) $\mathbf{I} = [I_1 \ I_2 \ \dots \ I_M]^T$ can be calculated using the following equation:

$$\mathbf{Z}\mathbf{I} = \mathbf{V} \quad (6)$$

where \mathbf{Z} is the mutual impedance matrix, which can be calculated using the induced electromotive force method as presented in [19].

$$\mathbf{Z} = \begin{bmatrix} Z_{11} & Z_{12} & \dots & Z_{1M} \\ Z_{21} & Z_{22} & \dots & Z_{2M} \\ \dots & \dots & \dots & \dots \\ Z_{M1} & Z_{M2} & \dots & Z_{MM} \end{bmatrix} \quad (7)$$

where Z_{mn} is the mutual impedance between elements m and n in the array, and is defined as follows [19]:

$$\mathbf{Z}_{mn} = \begin{cases} 73,1291 + 42,5446j & \text{if } m = n \\ 30[2C_i(u_0) - C_i(u_1) - C_i(u_2)] & \\ -30j[2S_i(u_0) - S_i(u_1) - S_i(u_2)] & \text{if } m \neq n \end{cases} \quad (8)$$

where: $u_0 = 2\pi d$; $u_1 = 2\pi\sqrt{d^2 + 0,25} + \pi$; $u_2 = 2\pi\sqrt{d^2 + 0,25} - \pi$; d is the distance between the antenna elements; C_i and S_i is calculated as follows:

$$\begin{aligned} C_i(u) &= \int_{-\infty}^u \frac{\cos(x)}{x} dx \\ S_i(u) &= \int_{-\infty}^u \frac{\sin(x)}{x} dx \end{aligned} \quad (9)$$

It can be observed from equations (6), (7), and (8) that the mutual impedance matrix \mathbf{Z} is not a diagonal matrix because $Z_{mn} \neq 0$ for $m \neq n$. Consequently, the effective input currents \mathbf{I} do not fully follow the voltage laws \mathbf{V} , which introduces distortions in the radiation pattern of the array, including the null depth level.

III. CONSTRAINT HANDLING TECHNIQUES

Optimization problems permeate every facet of applied sciences and engineering disciplines. The majority of practical applications require the restriction of physical variables, incorporating both equality and inequality constraints. Numerous methods exist for managing constraints [11], but two frequently employed strategies are penalty functions and the decoupling of the objective function from the constraints. In mathematical terms, the problem of constrained optimization can be expressed as described by [20]:

$$\begin{aligned} \text{Minimize } & f(x) \\ & g_j(x) \leq 0, j = 1, 2, \dots, j, \\ \text{subject to } & h_k(x) = 0, k = 1, 2, \dots, K, \\ & x_i^l \leq x_i \leq x_i^u, i = 1, 2, \dots, n, \end{aligned} \quad (10)$$

where:

- $f(x)$: The objective function concerning the vector variable x .
- $g_j(x)$: The inequality constraints.

- $h_k(x)$: The equality constraints.
- x_i', x_i'' represents the lower and upper limit values, respectively, of component x_i in x .

To solve this optimization problem, the article applied the APT and the OFRT [3]. Then, the constrained optimization problem (10) is transformed into an unconstrained optimization problem [21].

A. Adaptive Penalty Techniques (APT)

The APT transforms the constrained problem into an unconstrained one by incorporating a penalty term into the fitness function. This penalty term depends on the degree of constraint violations and the penalty factors, which may vary during the optimization process. The following general format can be used to formulate the modified objective function [3]:

$$F(x) = f(x) \pm \left[\sum_{j=1}^J r_j \cdot g_j(x) + \sum_{k=1}^K c_k \cdot h_k(x) \right] \quad (11)$$

With $F(x)$ represents the penalized objective function, also referred to as the fitness function, r_j and c_k are positive weighting coefficients referred to as penalty factors.

By transforming the equality constraints into inequality constraints, particularly beamforming techniques, equation (11) can be revised as [3]:

$$F(x) = f(x) \pm \sum_{j=1}^m r_j \cdot g_j(x) \quad (12)$$

In 2019, Kawachi *et al.* [22] introduced an adaptive method to determine the penalty factor (PF) dynamically throughout the evolutionary process, aiming to address concerns related to excessive or insufficient penalization that could cause the search process to stray from the optimal solution. Specifically, they formulated an objective function:

$$F(x) = f(x) \pm PF \cdot \bar{v}(x) \quad (13)$$

where $\bar{v}(x)$ represents the mean constraint violation, and PF denotes the penalty factor, and then three steps are carried out:

- **Step 1:** By comparing the following two individuals, the candidates for punishment factors $PFCs$ are identified:

$$PFC_{k,l} = -\frac{f(x_k) - f(x_l)}{\bar{v}(x_k) - \bar{v}(x_l)} \quad (14)$$

where, k and l indicate two different individuals; $PFCs$ is determined for all feasible combinations within a given population.

- **Step 2:** The penalty factor is established as follows: if the proportion of negative $PFCs$ surpasses 50%, the PF retains its previous generation's value;

alternatively, PF is computed as the average of the positive $PFCs$.

- **Step 3:** PF is revised. If the ratio of feasible individuals rf in the population surpasses p_{feas} , then the penalty factor for the next generation is determined as follows [3]:

$$PF_{G+1} = p_{rate} \cdot PF_G \quad (15)$$

where $p_{rate} \in [0,1]$ and the parameters are defined by the user, p_{feas} .

B. Original Feasibility Rules Technique (OFRT)

In the APT, it is necessary to experiment with various penalty factor values to determine the optimal choice, as incorrect values may lead to the divergence of the search process from the vicinity of the optimal solution. Deb (2000) introduced a new technique aimed at overcoming this limitation, which centers on a tournament selection operator to compare two solutions. The following rules are used [3]:

- for viable solution and non-viable solution, the feasible one is selected.
- for two viable solutions, the one with the superior objective function value is chosen.
- for between two non-viable solutions, the one with the lower violation parameter value is chosen.

In accordance with the initial feasibility rules technique, the fitness function is defined as follows:

$$F(x) = \begin{cases} f(x) & \text{if } g_j(x) \leq 0 \forall j=1,2,\dots,m \\ f_{\max} + \sum_{j=1}^m \max\{0, g_j(x)\} & \text{otherwise} \end{cases} \quad (16)$$

where the value of the objective function for the least advantageous viable option among the current population is denoted by f_{\max} . If a population has no workable solutions, f_{\max} is set to zero.

Using this method, each instance of a constraint violation is added together and evaluated as a single number. As a result, in the case of infeasible solutions, their evaluation is limited to the degree of constraint violation.

IV. PROPOSAL OF THE BEAMFORMER

Considering the objectives and criteria for interference suppression, the proposed beamformer needs to effectively mitigate interference while maintaining the main beam's direction and width and ensuring that the sidelobes remain within specified levels. The proposed beamformer is based on CHT, GWO, and complex weight control.

The formulation of the optimal complex weight vector for the described in Eq. (4), employing the CHTs and GWO-based approach, is as follows:

$$\mathbf{w}_o = \mathbf{w}_{\text{ref}} - \Delta \quad (17)$$

where:

- \mathbf{w}_{ref} : represents the reference weight vector, which is generated using methods such as the Chebyshev technique.
- \mathbf{w}_o : optimal weight vector
- Δ : the disturbance of the weight vector
- The optimized pattern, with enforced nulls, preserved main lobes and suppressed sidelobes, is depicted as:

$$P_o(\theta) = EF(\theta)\mathbf{s}(\theta)\mathbf{w}_o = EF(\theta)\mathbf{s}(\theta)(\mathbf{w}_{\text{ref}} - \Delta) \quad (18)$$

$$\Leftrightarrow P_o(\theta) = EF(\theta)\mathbf{s}(\theta)\mathbf{w}_{\text{ref}} - EF(\theta)\mathbf{s}(\theta)\Delta \quad (19)$$

$$\Leftrightarrow P_o(\theta) = EF(\theta)AF_{\text{ref}}(\theta) - EF(\theta)\mathbf{s}(\theta)\Delta \quad (20)$$

To impose K nulls in the direction of interferences for $k = 1, \dots, K$, where NDL is to be less than or equal to S_{dB} from the peak of the main lobe, then the resulting equations are formulated as:

$$\|\mathbf{S}\Delta - \mathbf{v}_{\text{ref}}\| \leq Thr \quad (21)$$

where:

$$Thr = 10 \frac{-S_{\text{dB}} + 20 \log_{10}(P_{\text{ref}}(\theta_0, \phi_0))}{20} \quad (22)$$

$$\mathbf{S} = \begin{bmatrix} \mathbf{s}(\theta_1)_1 & \dots & \mathbf{s}(\theta_1)_M \\ \mathbf{s}(\theta_2)_1 & \dots & \mathbf{s}(\theta_2)_M \\ \vdots & \ddots & \vdots \\ \mathbf{s}(\theta_K)_1 & \dots & \mathbf{s}(\theta_K)_M \end{bmatrix}. \quad (23)$$

$$\Delta = [\Delta_1, \dots, \Delta_M]^T \quad (24)$$

$$\mathbf{v}_{\text{ref}} = [AF_{\text{ref}}(\theta_1), \dots, AF_{\text{ref}}(\theta_K)]^T \quad (25)$$

Therefore, the optimization problem can be expressed as:

$$\begin{aligned} \min_{\Delta} \quad & \|\Delta\|_2 \\ \text{s.t.} \quad & \max(\|\mathbf{S}\Delta - \mathbf{v}_{\text{ref}}\|) - Thr \leq 0 \end{aligned} \quad (26)$$

This problem can be solved by CHT and GWO to acquire the optimal weight for the desired pattern.

For this paper:

$$\begin{aligned} f(x) &= \|\Delta\|_2 \\ v(x) &= \max(\|\mathbf{S}\Delta - \mathbf{v}_{\text{ref}}\|) \leq Thr \end{aligned} \quad (27)$$

In line with the objective of suppressing interference, the beamformer is engineered to possess interference suppression capabilities while preserving the direction and width of the main beam and controlling the sub-beam within predefined thresholds. Consequently, the challenge at hand manifests as a constrained optimization problem. Drawing from this assessment, the problem can be reformulated as an unconstrained optimization problem by employing two constraint processing techniques, namely

APT and OFRT, with the fitness function outlined as follows:

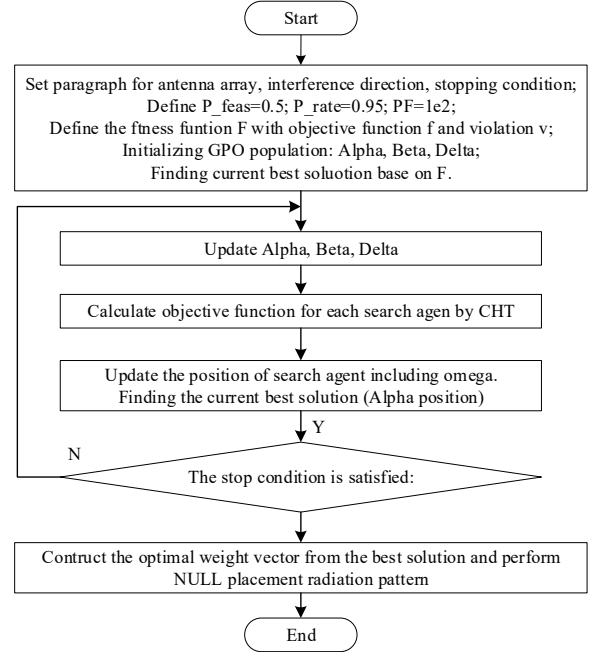


Fig. 3. Flowchart of the solution based on the GWO and CHTs.

The fitness function of the problem is rewritten by applying APT as follows:

$$F = \begin{cases} \|\Delta\|_2 & \text{if } v \leq 0 \\ \|\Delta\|_2 + PF \max(\|\mathbf{S}\Delta - \mathbf{v}_{\text{ref}}\|) - Thr & \text{if } v > 0 \end{cases} \quad (28)$$

The fitness function of the problem is rewritten by applying OFRT as follows:

$$F = \begin{cases} \|\Delta\|_2 & v \leq 0 \\ f_{\text{max}} + \max(\|\mathbf{S}\Delta - \mathbf{v}_{\text{ref}}\|) - Thr & v > 0 \end{cases} \quad (29)$$

In which: f_{max} is the largest value among the f target values found.

Initializations:

- The initial setup involves defining input data such as the number of array elements N , Max_I or the desired value of the fitness function, threshold, the Direction of Arrival (DOA) of interferences, the stopping condition (either the maximum number of iterations), and the radiation pattern of the array element.
- Define the objective function $f(x)$ and constraint function $v(x)$ from Eq. (27), in which the array factor is selected according to a specific pattern nulling technique as described in Eq. (1).
- Mapping solutions (sets of weights) to locations (x) of wolves in the population during the optimization process.

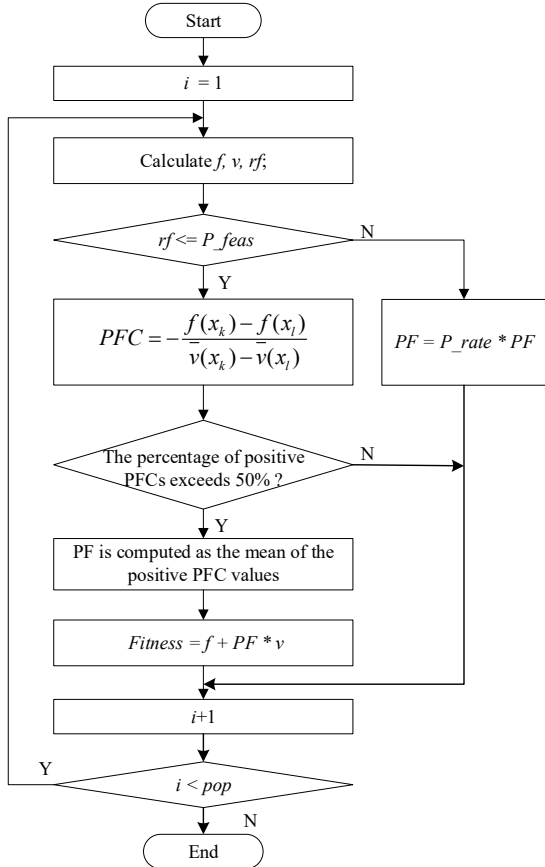


Fig. 4. Flowchart of the solution based on the APT.

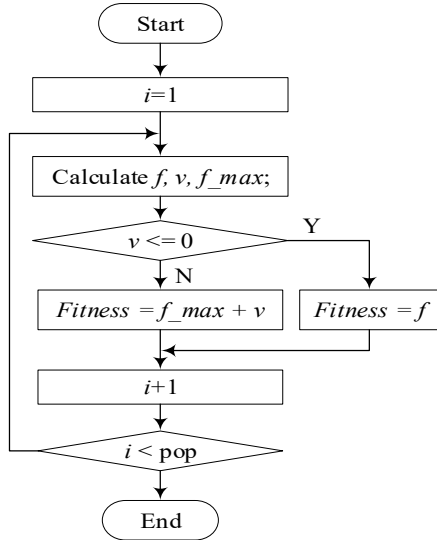


Fig. 5. Flowchart of the solution based on the OFRT.

Calculate fitness function by CHTs

The approach used to compute the fitness function using the ADP is detailed in the algorithm flowchart shown in Fig. 4, as is the technique employed to compute the fitness function using the OFRT, which is explained in detail in the algorithm flowchart presented in Fig. 5.

Finding the best solution by GWO:

The beamformer iteratively computes and explores the current optimal solution using the GWO method outlined

in [15]. The process persists until the termination criterion is satisfied. Subsequently, the final optimal solution is acquired.

Construction of array element weights:

The beamformer establishes the corresponding weights for every ULA element based on the ultimate optimal solution. Pattern nulling will be carried out using these weights.

V. NUMERICAL RESULT

The paper will consider five scenarios to evaluate CHTs based on the beamformer's ability to suppress interference. This involves processing the complex weights of the excitation signal for each individual element in the antenna array using a metaheuristic algorithm. The proposed method will be applied and evaluated on both the receiver and transmitter sides.

All scenario simulations will adhere to specified parameters, including the use of a 20-element half-wavelength dipole array, a GWO algorithm with a population size of 100, 200 Monte Carlo simulations, and a maximum of 200 iterations. The reference pattern will be generated using weights derived from the Chebyshev method with a sidelobe level (SLL) of -30 dB. Findings for all scenarios will be averaged from 50 simulations conducted in MATLAB 2023b, running on an Intel (R) Core (TM) i5-8265U CPU @ 1.60GHz.

In uniformly spaced arrays, the Chebyshev array's distinct weight distribution results in an optimal radiation pattern that effectively balances sidelobe levels and provides an ideal beamwidth, particularly at the first null point of the main beam [23]. Therefore, the Chebyshev array factor has been selected as the preferred pattern for this paper to manage the SLL and the main beam's beamwidth. In (1), the step size is fixed to $\theta = 1^\circ$.

Figs. 3–5 illustrate the flowcharts representing these solutions. Scenario 1, titled “Convergence Rate,” was employed to assess the time taken for the objective function to converge using the APT and OFRT. Subsequently, Scenarios 2-5 were utilized to evaluate the ability of the waveform generator to steer nulls, employing either the APT or the OFRT. The simulation outcomes for all scenarios are illustrated in Figs. 6–18.

A. Convergence Rate

This scenario compares the convergence performance of a beamformer using a GWO-based APT with the convergence speed of an adaptive beamformer using a GWO-based OFRT in the case of placing a null ($\theta = 20^\circ$), multiple nulls ($\theta = -20^\circ, 20^\circ, 40^\circ$) and wide nulls ($\theta = 20^\circ \div 40^\circ$) at the top of the side beams of the Chebyshev radiation pattern. The objective function value and violation value changing through each iteration are illustrated in Figs. 6–8 for the three cases of a single null, multiple nulls, and a broad null. It can be seen that the case of beamforming using the APT reaches the convergence point faster than the adaptive beamforming case using the OFRT. However, a larger population size results in

increased computation time. Therefore, a population size of 100 and 200 iterations will be selected to simulate the scenarios. With the ability to achieve such fast convergence, the APT can be a potential technique for real-time applications of radio communication systems.

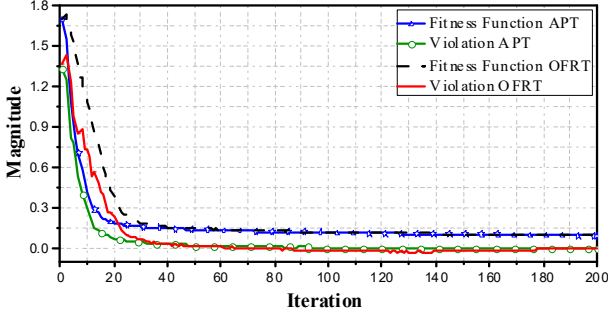


Fig. 6. The objective function and violation versus the number of iterations for the cases of a single null with $\theta = 20^\circ$.

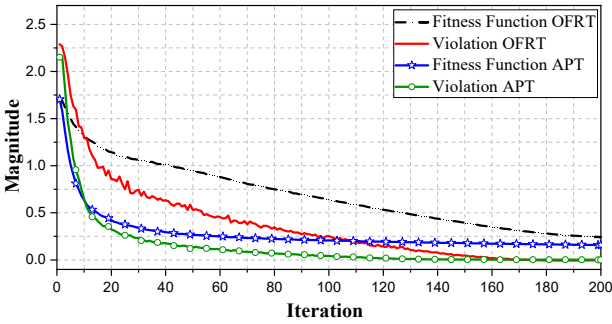


Fig. 7. The fitness function and violation versus the number of iterations for the cases of multiple nulls with $\theta = -20^\circ, 20^\circ, 40^\circ$.

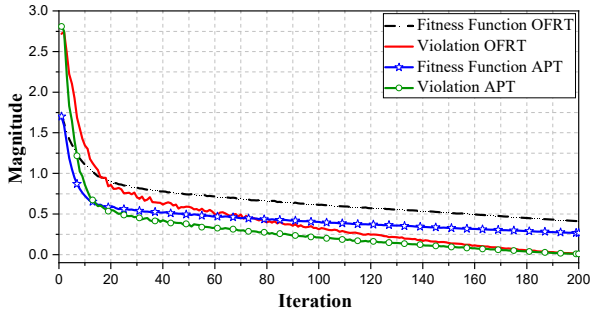


Fig. 8. The objective function and violation versus the number of iterations for the cases of a broad null with $\theta = 20^\circ \div 40^\circ$.

In scenario 2, we will compare and evaluate the possibility of placing a null on the radiation pattern of APT and OFRT. The null can be positioned in any direction. In this instance, it is selected to align with the top of the third sidelobe (20°). We initialize the individuals with Chebyshev array weights, ensuring a SLL of -30 dB.

B. Ability to Eliminate Interferences

Fig. 9 depicts the optimized radiation patterns featuring a single null value achieved through the APT and the OFRT. It is evident that the optimal radiation patterns by both APT and OFRT have preserved most of the characteristics of the Chebyshev radiation pattern, such as the main beam direction, FNBW ($FNBW = 18^\circ$), HPBW ($HPBW = 6^\circ$), and SLL ($SLL = -30$ dB) except that the

NDL at 20° is -49.595 dB and -49.978 dB for the APT and OFRT, respectively. Fig. 10 further elucidates this result, demonstrating the close proximity between the cumulative distribution function (CDF) curves of the SLLs in the radiation diagram using the APT, the OFRT, and Chebyshev’s pattern. These results clearly demonstrate the significant interference suppression effect achieved by precisely placing a null point in the noise direction using CHTs.

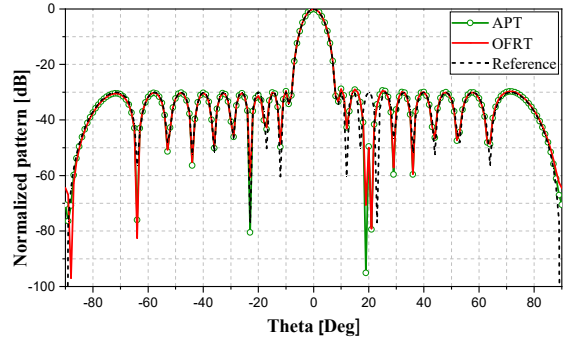


Fig. 9. Optimized pattern with a single null at 20° .

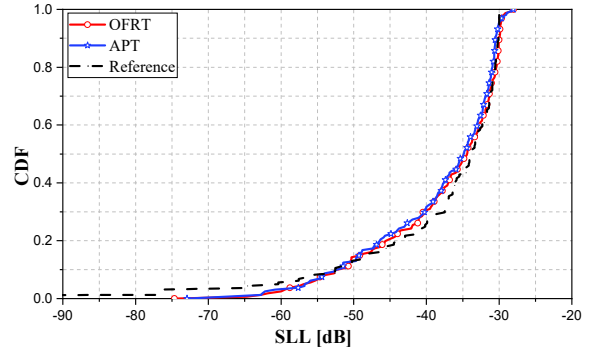


Fig. 10. CDFs of SLLs for the cases of a single null with $\theta = 20^\circ$.

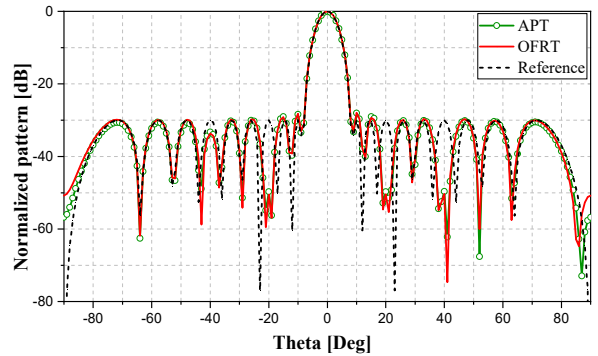


Fig. 11. Optimized pattern with three nulls at $-20^\circ, 20^\circ$, and 40° .

Scenario 3 refines the radiation pattern by combining multiple individual nulls situated at angles of $-20^\circ, 20^\circ$, and 40° . The optimized radiation patterns with multiple nulls, shown in Fig. 11 were created using the APT and OFRT. These methods effectively maintain nearly all the attributes of the original Chebyshev pattern, except that the sidelobe at -40° exhibits an SLL of approximately -35 dB. The null depth levels at $-20^\circ, 20^\circ$, and 40° are as follows: -49.691 dB, -49.682 dB, and -49.653 dB with the APT, and -50.508 dB, -50.433 dB, and -50.327 dB with the OFRT, respectively. This is evident in Fig. 11,

which demonstrates that all NDL values are deep at the -50 dB threshold and all SLL values closely follow the -30 dB threshold, while maintaining the HPBW close to the Chebyshev pattern. These results are shown more clearly in Fig. 12, where the two CDF lines of the SLLs of the radiation diagram using the APT and the radiation diagram using the OFRT closely follow the CDF line of the SLL of the Chebyshev radiation diagram. This scenario further illustrates the noise suppression and interference mitigation capabilities of CHTs.

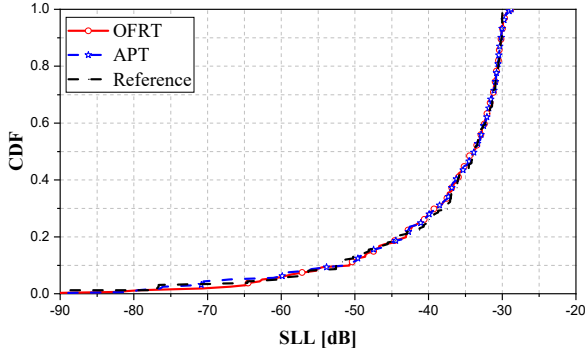


Fig. 12. CDFs of SLLs for the cases of multiple nulls with $\theta = -20^\circ, 20^\circ, 40^\circ$.

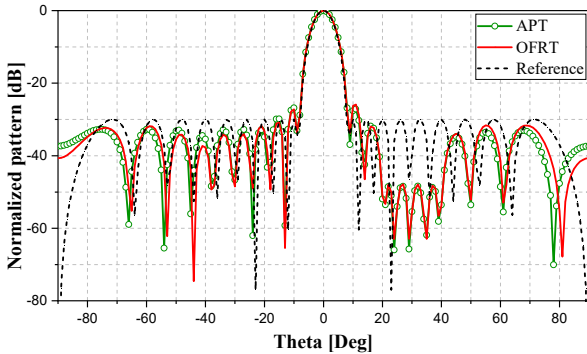


Fig. 13. The optimized pattern exhibits a broad null spanning from 20° to 40° .

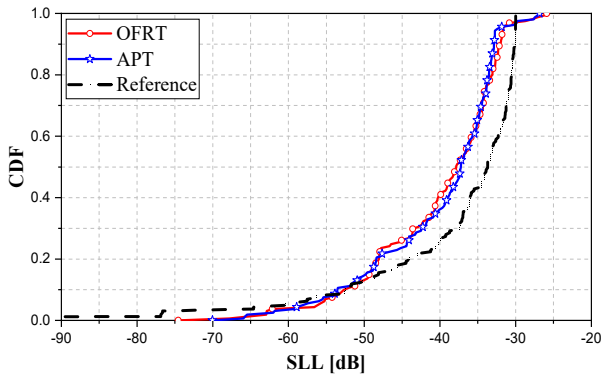


Fig. 14. CDFs of SLLs for the cases of a broad null with $\theta = 20^\circ \div 40^\circ$.

To demonstrate the capacity for broad interference suppression, Scenario 4 involves generating a pattern with a broad null imposed to cover the target sector of $[20^\circ, 40^\circ]$. This pattern is depicted in Fig. 13. The main beam width remains virtually unchanged, and the maximum SLL is approximately -30 dB. The results demonstrate that the ability to synthesize radiation patterns using APT and

OFRT is still superior. The results are illustrated more clearly in Fig. 14.

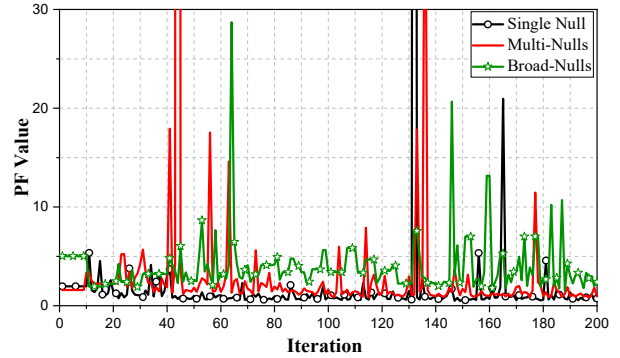


Fig. 15. PF value through each iteration with a single null, three nulls, and a broad null.

The graph in Fig. 15 depicts the change in the value of the PF corresponding to each iteration of the APT. In the graph, there are three lines representing the change of PF through each loop, corresponding to three cases: a single null, multiple nulls, and a wide null. The graph clearly shows that the PF value gradually decreases with each iteration, reaching a plateau. However, there are a few spikes in some iterations, but the PF then returns to stability and continues to decrease. This illustration shows that changes in the PF value reflect the refinement of the constraint handling technique, particularly the APT, which is adjusted to suit each stage of the optimization problem. Thus, the graph depicting the change in PF provides insight into the effectiveness of the APT in solving optimization problems.

C. Patterns with Mutual Coupling

Scenario 5 investigates the impact of mutual coupling on the optimal radiation pattern obtained using the APT-GWO method. The mutual coupling effect is quantified through the mutual impedance matrix discussed in Section II. This impact is analyzed for scenarios involving the placement of a single null at 20° , with null thresholds set at -50 dB, -60 dB, -70 dB, -80 dB, and -90 dB. For a detailed analysis, Fig. 16 presents the simulation results for a single null at 20° with a null threshold of -50 dB. The results demonstrate that the null points were accurately placed at the predefined locations, though with reduced null depth levels. The CDF in Fig. 17 further shows that the APT method without mutual coupling (No MC) achieves lower SLLs, indicating more effective side lobe suppression. However, when mutual coupling (MC) is considered, the performance of the APT method is significantly compromised, both in terms of null placement precision and side lobe level control. Fig. 18 depicts the simulation results for the specific case of a single null at 20° with a null threshold of -90 dB, while the remaining results are summarized in Table I. The findings reveal that although the null points were accurately positioned at the desired locations, the null depth levels were shallower, and controlling the side lobes at -30 dB proved challenging, despite the main lobe being well maintained.

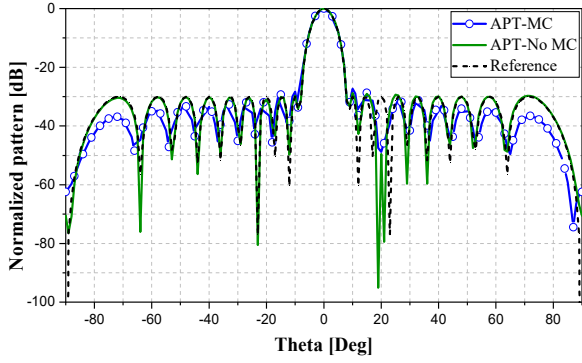


Fig. 16. Optimized patterns when considering mutual coupling effects (null at 20° and null threshold set at -50 dB).

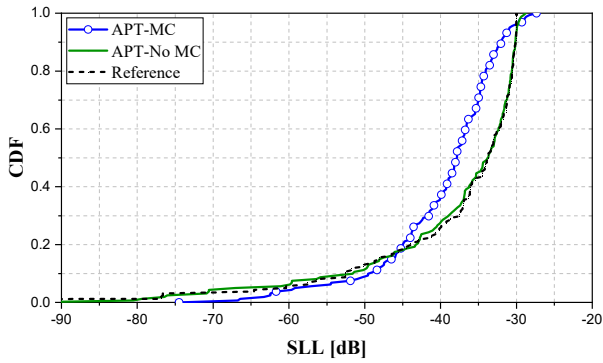


Fig. 17. CDFs of SLLs for scenarios with and without mutual coupling effects (null at 20° and null threshold set at -50 dB).

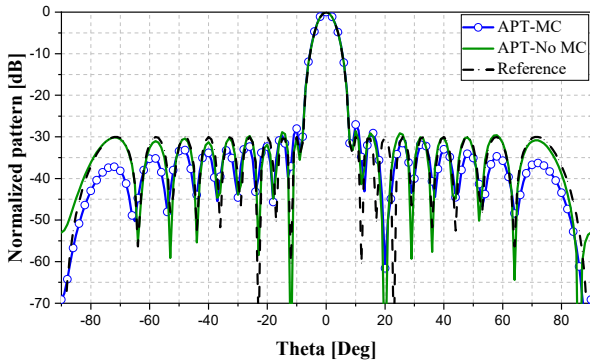


Fig. 18. Optimized patterns when considering mutual coupling effects (null at 20° and null threshold set at -90dB).

TABLE I. NDL AT 20° WITH AND WITHOUT MUTUAL COUPLING EFFECTS

Threshold	NDL (dB)	
	No MC	MC
-50 dB	-49.595	-48.88
-60 dB	-59.93	-55.01
-70 dB	-69.95	-59.19
-80 dB	-79.98	-61.86
-90 dB	-90.21	-61.58

VI. CONCLUSION

Our paper presents a novel beamforming approach utilizing GWO in conjunction with two CHTs, namely APT and OFRT, for interference suppression in ULA. Through evaluation across five scenarios-including convergence rate, placing single null, multiple nulls, and

broad nulls on the radiation pattern in an ideal case, and the impact of interference-we demonstrate the efficacy of APT and OFRT in mitigating interference while maintaining main lobe width and sidelobe levels. Our results indicate that configurations employing APT consistently outperform those utilizing OFRT across all evaluated metrics. This underscores the potential of APT as a promising solution for interference suppression in radio communication systems employing smart antennas like 5G and radar.

Furthermore, we emphasize the significance of CHTs as powerful tools to harness metaheuristic algorithms for solving constraint optimization problems effectively. Looking forward, we plan to explore alternative CHTs such as the ϵ -constrained method or the stochastic ranking method to address challenges posed by unknown noise directions in future research endeavors, thereby enhancing the capabilities of advanced antenna systems in interference mitigation.

CONFLICT OF INTEREST

The authors declare no conflict of interest.

AUTHOR CONTRIBUTIONS

All authors conducted the research; simulated and analyzed the data; wrote the paper, and all authors had approved the final version.

REFERENCES

- [1] H. L. Van Trees, "Optimum array processing: Part IV of detection, estimation, and modulation theory," *New York, NY, USA: Wiley*, pp. 1-12, 2002.
- [2] R. L. Haupt, "Antenna arrays: A computational approach," *Hoboken, NJ, USA: Wiley*, pp. 156-176; 484-515, 2010.
- [3] N. D. Lagaros, M. Kourmoutos, and N. A. Kallioras, "Constraint handling techniques for metaheuristics: a state-of-the-art review and new variants," *Optim Eng*, vol. 24, pp. 2251-2298, 2023.
- [4] T. V. Luyen, L. V. Thai, N. M. Tran, and N. V. Cuong, "Reconfigurable intelligent surface-aided wireless communication considering interference suppression," *Ad Hoc Networks. Lecture Notes of the Institute for Computer Sciences, Social Informatics and Telecommunications Engineering*, vol. 558, pp. 86-98, 2024.
- [5] D. E. Goldberg, "Genetic algorithms in search, optimization & machine learning," *Addison-Wesley*, 1989, p. 401. Print ISSN:0912-8085, 1986-2013.
- [6] K. Deb, *Multiobjective Optimization Using Evolutionary Algorithms*, John Wiley and Sons Ltd, KanGAL Report Number 2011003, 2011.
- [7] K. X. Thuc, H. M. Kha, N. V. Cuong, and T. V. Luyen, "A metaheuristics-based hyperparameter optimization approach to beamforming design," *IEEE Access*, vol. 11, pp. 52250-52259, 2023.
- [8] E. G. Talbi, *Metaheuristics: From Design to Implementation*, John Wiley & Sons, 2009.
- [9] C. A. Coello Coello, G. B. Lamont, and D. A. Van Veldhuizen, "Evolutionary algorithms for solving multi-objective problems," *Springer Science & Business Media*, 2007.
- [10] A. E. Eiben and J. E. Smith, *Introduction to Evolutionary Computing*, Springer, 2015.
- [11] E. Mezura-Montes and C. A. C. Coello, "Constraint-handling in nature-inspired numerical optimization: Past, present and future," *Swarm Evol Comput*, vol. 1, no. 4, pp. 173-194, 2011.
- [12] R. Mallipeddi, S. Jeyadevi, P. N. Suganthan, and S. Baskar, "Efficient constraint handling for optimal reactive power dispatch problems," *Swarm Evol Comput*, vol. 5, pp. 28-36, 2012.

- [13] A. R. Jordehi, "A review on constraint handling strategies in particle swarm optimisation," *Neural Comput Appl*, vol. 26, no. 6, pp. 1265-1275, 2015.
- [14] X. Lin, W. Luo, Y. Qiao, P. Xu, and T. Zhu, "Empirical study of population-based dynamic constrained multimodal optimization algorithms," in *Proc. 2019 IEEE Symposium Series on Computational Intelligence*, 9002835, pp. 722-730, SSCI 2019.
- [15] S. Mirjalili, S. M. Mirjalili, and A. Lewis, "Grey wolf optimizer," *Advances in Engineering Software*, vol. 69, pp. 46-61, 2014.
- [16] L. Tong and C. Nguyen, "An effective beamformer for interference suppression without knowing the direction," *International Journal of Electrical and Computer Engineering (IJECE)*, vol. 13, no. 1, pp. 601-610, 2023.
- [17] V. L. Tong, M. K. Hoang, T. H. Duong, T. Q. T. Pham, V. T. Nguyen, and V. B. G. Truong, "An approach of utilizing binary bat algorithm for pattern nulling," *Springer Singapore*, 2020.
- [18] L.T. Trang, N. V. Cuong, and T. V. Luyen, "Interference suppression approaches utilizing phase-only control and metaheuristic algorithms: A comparative study," *Ad Hoc Networks. Lecture Notes of the Institute for Computer Sciences, Social Informatics and Telecommunications Engineering*, vol. 558, pp. 65-85, 2024.
- [19] Constantine A. Balanis, *Antenna Theory: Analysis and Design*, Hoboken, NJ: John Wiley & Sons, 4th ed, pp. 933-943, 2016.
- [20] K. Deb, "An efficient constraint handling method for genetic algorithms," *Comput Methods Appl Mech Eng*, vol. 186, pp. 311-338, 2000.
- [21] Yang, Xin-She, *Nature-inspired Optimization Algorithms*, Academic Press, 2020.
- [22] T. Kawachi, J. I. Kushida, A. Hara, and T. Takahama, "Efficient constraint handling based on the adaptive penalty method withbalancing the objective function value and the constraint violation," in *Proc. 2019 IEEE 11th International Workshop on Computational Intelligence and Applications*, 2019, pp. 121-128.
- [23] C. L. Dolph, "A current distribution for broadside arrays which optimizes the relationship between beam width and side-lobe level," in *Proc. IRE*, Jun. 1946, vol. 34, no. 6, pp. 335-348.

Copyright © 2024 by the authors. This is an open access article distributed under the Creative Commons Attribution License ([CC BY-NC-ND 4.0](https://creativecommons.org/licenses/by-nc-nd/4.0/)), which permits use, distribution and reproduction in any medium, provided that the article is properly cited, the use is non-commercial and no modifications or adaptations are made.